BIOCHEMISTRY
including biophysical chemistry & molecular biology

Article

pubs.acs.org/biochemistry

Structural Effects of Two Camelid Nanobodies Directed to Distinct C-Terminal Epitopes on α-Synuclein

Farah El-Turk,[§,‡] Francisco N. Newby,[§] Erwin De Genst,[§] Tim Guilliams,[§,†] Tara Sprules,[‡] Anthony Mittermaier,[‡] Christopher M. Dobson,[*,§] and Michele Vendruscolo[*,§]

[§]Department of Chemistry, University of Cambridge, Cambridge CB2 1EW, U.K.
[‡]Department of Chemistry, McGill University, Montreal, Quebec H3A 2K6, Canada

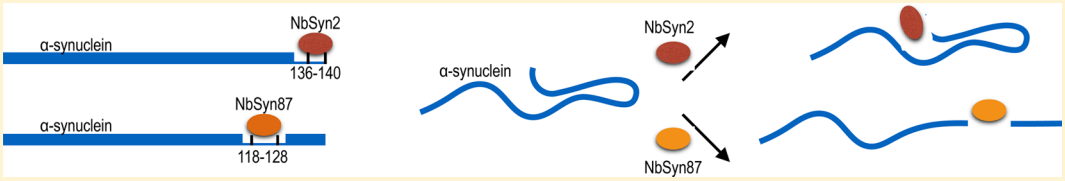

ABSTRACT: α-Synuclein is an intrinsically disordered protein whose aggregation is associated with Parkinson's disease and other related neurodegenerative disorders. Recently, two single-domain camelid antibodies (nanobodies) were shown to bind α-synuclein with high affinity. Herein, we investigated how these two nanobodies (NbSyn2 and NbSyn87), which are directed to two distinct epitopes within the C-terminal domain of α-synuclein, affect the conformational properties of this protein. Our results suggest that nanobody NbSyn2, which binds to the five C-terminal residues of α-synuclein (residues 136−140), does not disrupt the transient long-range interactions that generate a degree of compaction within the native structural ensemble of α-synuclein. In contrast, the data that we report indicate that NbSyn87, which targets a central region within the C-terminal domain (residues 118−128), has more substantial effects on the fluctuating secondary and tertiary structure of the protein. These results are consistent with the different effects that the two nanobodies have on the aggregation behavior of α-synuclein in vitro. Our findings thus provide new insights into the type of effects that nanobodies can have on the conformational ensemble of α-synuclein.

α-Synuclein is a 140-residue protein that plays a pivotal role in the etiology of a set of neurodegenerative disorders associated with protein aggregation and amyloid formation collectively known as synucleinopathies, of which the most common is Parkinson's disease.[1−8] Parkinson's disease is characterized by the accumulation of α-synuclein in intracellular inclusions, known as Lewy bodies, located in the brain stems of affected patients, as well as by a loss of dopaminergic neurons in the *substantia nigra pars compacta*.[1−9] Extensive data indicate that pathogenicity is associated with early oligomeric aggregates of α-synuclein populated during the formation of Lewy bodies rather than by the characteristic amyloid fibrils observed in the late stages of the aggregation process.[10−12] Thus, a clear understanding of the physiological and pathophysiological states of α-synuclein is vital for the identification of novel diagnostic and therapeutic strategies to enable interventions to take place before irreversible cellular damage has occurred.

A potentially powerful therapeutic approach for reducing the risk of onset of synucleinopathies is to target the initial events in the aggregation process of α-synuclein to stabilize the soluble monomeric form and inhibit the formation of potentially harmful oligomeric assemblies[13] of the protein. This goal requires a systematic study of the intrinsic and extrinsic factors defining the initial events in the aggregation process and the identification of the specific structural features of α-synuclein in its monomeric state that modulate its aggregation behavior. One approach that we are exploring is based on the use of single antigen-binding domains of camelid antibodies, often known as nanobodies.[14−16] Their small size (∼14 kDa), high stability, high solubility, high level of production in recombinant hosts, and low level of immunogenicity (because of their high sequence similarity with the human VH family III) have prompted exploration of the use of nanobodies in both basic research and clinical studies designed to ameliorate neurodegenerative conditions.[14,16−20]

The work discussed in the present study focuses on two nanobodies, NbSyn2 and NbSyn87, which have been raised specifically against monomeric α-synuclein through an immunization and phage-display selection strategy.[15,21] Both NbSyn2 and NbSyn87 recognize with midnanomolar affinity specific regions within the C-terminal domain of the intrinsically disordered protein between residues 136 and 140 (K_D = 100 nM at 20 °C) and between residues 118 and 131 (K_D = 20 nM at 20 °C), respectively.[15,21] Herein, by comparing the effects of binding of these two nanobodies to monomeric α-synuclein, we report how two specific sequences in the C-terminal domain of α-synuclein modulate in different manners the conformational sampling of the entire molecule.

Received: February 17, 2016
Revised: April 19, 2016
Published: April 20, 2016

DOI: 10.1021/acs.biochem.6b00149
Biochemistry 2016, 55, 3116−3122

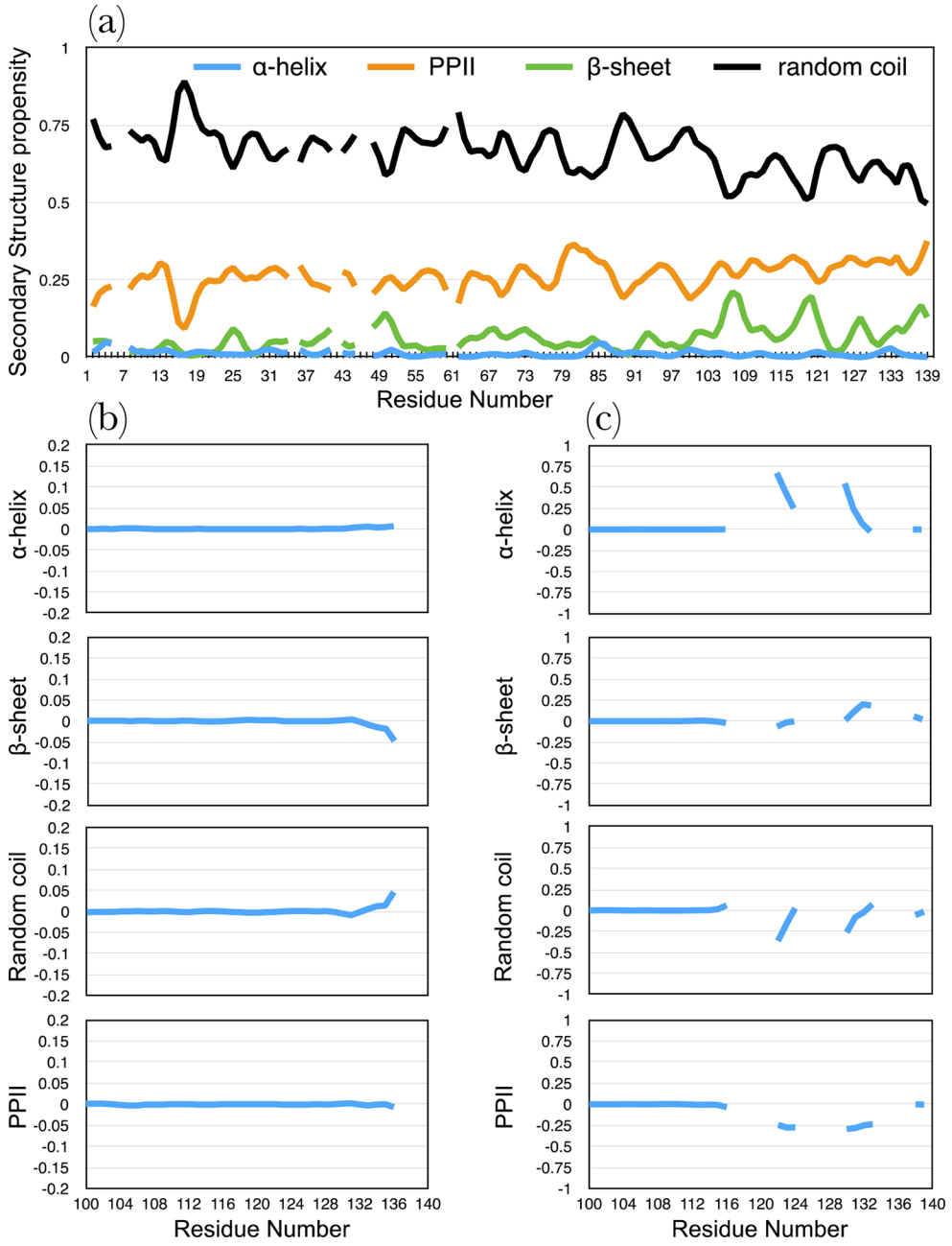

Figure 1. Secondary structure populations (calculated using the δ2D method[31]) of free α-synuclein (a). Changes in these populations in the presence of NbSyn2 (b) and NbSyn87 (c).

The epitope of NbSyn2 on α-synuclein has been previously characterized by NMR spectroscopy and X-ray crystallography.[15] The epitope of NbSyn87 has not been determined in similar detail, although binding of the nanobody to α-synuclein has been observed to lead to broadening and chemical shift perturbations of NMR resonances for residues located between V118 and A140.[15,21] Previous analyses have revealed that NbSyn87 recognizes a domain comprising residues 118−131[21] and that phosphorylation at S129 has no effect on the binding affinity of α-synuclein for NbSyn87. In contrast, phosphorylation at Y125 decreases the binding affinity significantly, consistent with the observation that the NbSyn87 epitope is located within the V118−P128 region.

MATERIALS AND METHODS

Chemicals. All chemicals and reagents were purchased from Sigma-Aldrich, U.K., unless otherwise stated. Protein concentrations were measured by UV absorbance spectroscopy using molecular extinction coefficients based on standard amino acid content with the ExPASy-ProtParam tool. The extinction coefficients at 280 nm of α-synuclein, NbSyn2, and NbSyn87 are 5960, 27180, and 26025 M^{-1} cm^{-1}, respectively.[15,21]

Expression and Purification of α-Synuclein. Expression and purification of the unlabeled ($^{14}N/^{12}C$), uniformly labeled ($^{15}N/^{12}C$), and double-labeled ($^{15}N/^{13}C$) α-synuclein were carried out as described previously.[15,21]

Expression and Purification of the Unlabeled Nanobodies NbSyn2 and NbSyn87. Expression and purification of nanobodies NbSyn2 and NbSyn87 were performed as

DOI: 10.1021/acs.biochem.6b00149
Biochemistry 2016, 55, 3116−3122

previously described.[15,21] Briefly, NbSyn2 and NbSyn87 were expressed in the periplasm of *Escherichia coli* strain WK6. The proteins were subsequently purified using immobilized metal (Ni) affinity chromatography followed by size-exclusion chromatography (Superdex 75 26/60). The purity and identity of the proteins were verified by sodium dodecyl sulfate−polyacrylamide gel electrophoresis (SDS−PAGE) and matrix-assisted laser desorption ionization time-of-flight (MALDI) spectroscopy. All proteins were found to be more than 98% pure. Mass spectrometry analysis revealed single peaks with the expected average molar mass: 14460, 14626, 15253, 14281, and 14098 Da for unlabeled $^{14}N/^{12}C$ α-synuclein, monolabeled $^{15}N/^{12}C$ α-synuclein, double-labeled $^{15}N/^{13}C$ α-synuclein, NbSyn2, and NbSyn87, respectively.

Aggregation Measurements. α-Synuclein samples (70 μM), freshly purified by gel filtration chromatography (Superdex 75 26/60) using PBS buffer, were incubated with and without nanobodies at 1/1 or 0.5/1 nanobody/α-synuclein molar ratios at 37 °C under continuous shaking at 200 rpm. Aliquots (7 μL) were removed every few hours, and 150 mM NaCl was added to give a final concentration of 2 μM. Aliquots were removed in triplicate and used to monitor the concentration of monomeric α-synuclein by dot-blot assays.

NMR Spectroscopy. NMR spectra were acquired at 283 K on a Varian INOVA 800 MHz spectrometer equipped with a cold probe. NMR data were subsequently processed using NMRpipe,[22] and SPARKY[38] was used for data analysis. Aggregation did not occur under these conditions (low temperature and absence of stirring). All experiments were performed in buffer A: 25 mM Tris, 100 mM NaCl, pH 7.4, and 5% D_2O (v/v).

Backbone Chemical Shift Measurements of Labeled α-Synuclein. Backbone assignments and chemical shift measurements were carried out using standard $^{15}N-^{1}H$ HSQC and triple-resonance 3-dimensional (3D) experiments, including HNCACB (complex points: 1666:H(F3)/180:C(F2)/72:N(F1)), HNCO (1666:H/40:C/72:N), and HNHA (1666:H/200:HA/72:N). The 200 μM α-synuclein samples in buffer A were prepared in the absence and presence of equimolar concentrations of unlabeled NbSyn2 or NbSyn87. DSS (4,4-dimethyl-4-silapentane-1-sulfonic acid) was used to calibrate the ^{1}H chemical shifts directly; calibrations of ^{13}C and ^{15}N chemical shifts were calculated according to their gyromagnetic ratios.[23]

Residual Dipolar Coupling (RDC) Measurements of Labeled α-Synuclein. Previously, highly reproducible RDC patterns were obtained for α-synuclein in both steric (*n*-octyl-penta(ethylene glycol)/octanol (C8E5)) and charged *Pf1* nematic liquid crystalline media at 100 mM NaCl in 10−15 mg mL^{-1} *Pf1* phage.[24,25] Our studies were therefore performed at the same ionic strength, and the absence of changes in chemical shifts indicates that the alignment medium used did not significantly perturb the conformational ensemble of α-synuclein.

RDCs were measured for samples of α-synuclein (200 μM) aligned in 15 mg/mL bacteriophage *Pf1* (ASLA Biotech) in buffer A. One-bond ^{15}N ^{1}H RDCs ($^{1}D_{NH}$) were determined by using an IPAP ^{15}N-HSQC sequence.[26] $^{1}D_{NH}$ values were calculated as the difference between the apparent scalar coupling in the presence of the alignment medium and that measured for an isotropic sample. One-bond $^{13}C\alpha$ $^{1}H\alpha$ dipolar couplings ($^{1}D_{C\alpha H\alpha}$) were determined using a modified 3D HN(CO)CA experiment where $^{13}C\alpha(i-1)$ ^{1}H coupling ($^{1}J_{C\alpha H\alpha}$ + $^{1}D_{C\alpha H\alpha}$) was permitted to evolve by removal of the proton refocusing pulse during the ^{13}C chemical shift evolution period. Experiments were performed on isotropic and aligned samples to calculate $^{1}D_{C\alpha H\alpha}$. The apparent scalar coupling $^{1}J_{C\alpha H\alpha}$ was allowed to evolve during non-constant time acquisition on Cα, which extends for a duration of ∼10 ms. Given that $^{1}J_{C\alpha C\beta}$ couplings are much smaller than $^{1}J_{C\alpha H\alpha}$ couplings, no splitting due to Cα Cβ was observed, and they could be ignored.[27,28] RDCs observed for α-synuclein under different conditions (free or nanobody bound) were normalized on the basis of the size of the splitting of the deuterium signal.

RESULTS

We used NMR spectroscopy to characterize the conformational properties of α-synuclein both when free and when in complex with the NbSyn2 and NbSyn87 nanobodies. No substantial changes in peak intensities and chemical shifts were observed in 2-dimensional (2D) $^{1}H/^{15}N$ correlation spectra upon binding either nanobody other than for signals previously shown to originate from the interaction site and neighboring amino acids (see Materials and Methods). We could, however, observe differences in other backbone chemical shifts ($^{13}C\alpha$, $^{13}C\beta$, ^{13}CO, and $^{1}H\alpha$) which are more sensitive to changes in secondary structure.[29,30] We used these chemical shift perturbations to investigate the effects of nanobody binding on the secondary structure populations of α-synuclein. To this end, we applied the δ2D method, which translates a set of backbone chemical shifts into secondary structure populations.[31] The results of the δ2D method for α-synuclein are consistent with it being an intrinsically disordered protein (Figure 1a), as all residues have a propensity for random coil conformations higher than 50% and a significant tendency to adopt the polyproline II (PPII) structure (∼25%), which has been shown to be important in stabilizing long-range interactions within α-synuclein.[32] The PPII content decreases when α-synuclein aggregates and is linked to an increase in β-sheet structure.[33] Slightly higher levels of secondary structure are observed at the C-terminus with about 5% more PPII, 20% more β-sheet content, and 10−20% less random coil in the vicinity of hydrophobic residues (G106, A107, V117, and M127). It is interesting that proline residues (P108, P120, P128, and P138) are within sequences with higher β-sheet propensity, suggesting that they could play a role in avoiding edge-to-edge association between soluble monomeric α-synuclein proteins that might promote aggregation.[34]

On the basis of the δ2D analysis, we found that neither of the nanobodies significantly affects the sampling of secondary structure of the protein in the N-terminal and NAC regions (see Materials and Methods). We observed, however, an increase in random coil propensity and a concomitant decrease in β-sheet propensity in a region near the binding epitope of NbSyn2 (residues 134−136) when this nanobody was bound (Figure 1b). In contrast, binding of NbSyn87, whose epitope is located near the center of the C-terminal region of α-synuclein (residues 118−128), resulted in a 20−70% increase in the α-helical population in the vicinity of residues 122−124 and 130−133 in combination with a 10−25% increase in β-sheet population for residues 130−133. This increase in order in the C-terminal domain is accompanied by a decrease in the content of random coil and PPII, suggesting that NbSyn87 enhances the structural compactness of α-synuclein at the C-terminus without leading to a stable folded structure (Figure 1c).

DOI: 10.1021/acs.biochem.6b00149
Biochemistry 2016, 55, 3116−3122

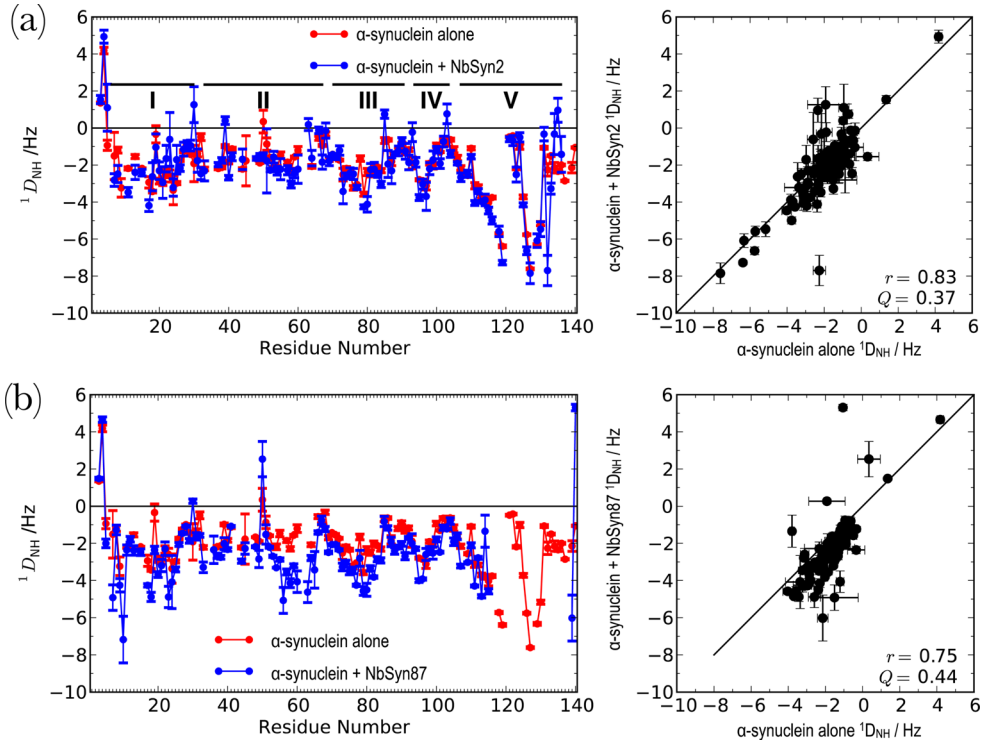

Figure 2. $^1D_{NH}$ values of free α-synuclein (red) and α-synuclein in the presence of equimolar concentrations of NbSyn2 (blue, a) and NbSyn87 (blue, b). Error bars represent a 95% confidence interval from four repeat measurements.

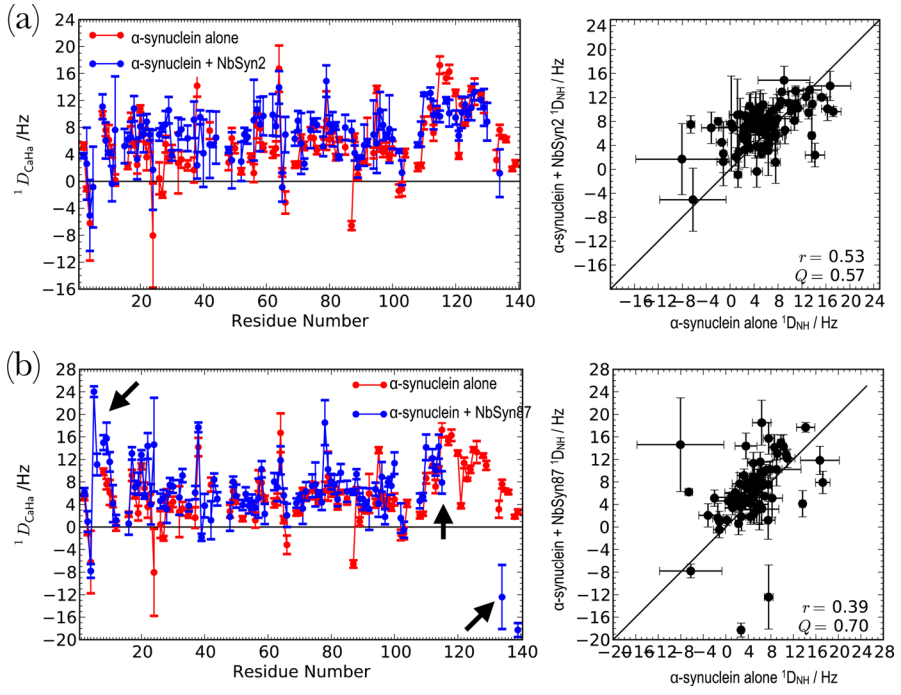

Figure 3. $^1D_{C\alpha H\alpha}$ of free α-synuclein (red) and α-synuclein in the presence of equimolar concentrations of NbSyn2 (blue, a) and NbSyn87 (blue, b). Error bars represent a 95% confidence interval from four repeat measurements.

RDCs measured for samples partially aligned in liquid crystalline media are a rich source of structural and dynamic information on unfolded proteins.[35,36] One-bond $^{15}N-^1H$ RDCs ($^1D_{NH}$) and $^{13}C\alpha$ $^1H\alpha$ RDCs ($^1D_{C\alpha H\alpha}$) were therefore measured for α-synuclein aligned in a suspension of filamentous bacteriophage *Pf1* (see Materials and Methods).

The $^1D_{NH}$ values for free α-synuclein are negative, indicating a preferential alignment of the NH bond vectors perpendicular to the magnetic field, a conclusion consistent with the protein being largely disordered.[24] Following previous studies, we identified five different domains within the protein sequence[24] (Figure 2a); three domains with relatively large negative RDCs were found at the N-terminal and NAC regions (domains I, III,

DOI: 10.1021/acs.biochem.6b00149
Biochemistry 2016, 55, 3116−3122

and IV), and another domain with particularly large values is located in the C-terminal region (domain V, Figure 2a). These site-specific differences in RDCs indicate variations in the rigidity of the polypeptide chain resulting from transient local secondary structure elements or long-range interactions.[24] In particular, the relative rigidity observed near domains I, II, III, IV, and V can be attributed to transient long-range interactions between the C-terminal region and the N-terminal and NAC regions.[24,36,37] In addition, enhanced rigidity at the C-terminal domain can be explained by a combination of long-range interactions and transient local secondary structure, particularly in the vicinity of residues 119 and 127 (Figures 1a and 2a). The five domains are flanked by regions with RDCs near zero, corresponding to residues with small side chains (A29, A30, A51, G67, G68, A85, and G86) that result in high flexibility of the protein backbone. Furthermore, the positive RDC values for the N-terminal residues V3 and F4 can be explained by residual electrostatic interactions of the N-terminus with the negatively charged *Pf1*.

We found that neither NbSyn2 nor NbSyn87 affects the overall pattern of the backbone $^1D_{NH}$ values, confirming that the protein remains disordered upon nanobody binding (Figures 2a and b). Nonetheless, subtle differences in the RDC patterns are observed for α-synuclein bound to both NbSyn2 and NbSyn87. No changes in the large negative $^1D_{NH}$ values are seen at the C-terminal domain of α-synuclein when bound to NbSyn2, while negligible decreases are observed for the N-terminal residues K12, E13, G14, and V15. These results indicate that NbSyn2 does not detectably affect the long-range interactions between the large acidic C-terminal domain and the positively charged N-terminal region. However, a slight increase in $^1D_{NH}$ values of residues in the vicinity of the binding site (residues 132−136) is observed. This finding agrees well with the δ2D results, indicating a modest increase in the protein flexibility at the C-terminus. In contrast, when α-synuclein is bound to NbSyn87, large changes in $^1D_{NH}$ values for residues E114, E139, and A140 in the C-terminal domain as well as substantial enhancements of the negative $^1D_{NH}$ values in domains I, II, and III are observed (Figure 2b), suggesting that the long-range interactions involving the C-terminal domain and the N-terminal and NAC regions are perturbed upon binding to the nanobody. Although the signals are too broad to observe for residues between V118 and P138, perturbations observed for residues E114 and E139 are likely to extend into this region in line with the conformational changes detected through the chemical shift measurements (Figure 1 and Materials and Methods).

$^1D_{C\alpha H\alpha}$ values yield important information about the orientation of the backbone structure outside the plane of the peptide bond and thus provide structural information about protein conformation complementary to that for $^1D_{NH}$ measurements. The $^1D_{C\alpha H\alpha}$ values for α-synuclein are largely small and positive, consistent with a highly unstructured polypeptide chain (Figure 3). Overall, the RDC patterns for free α-synuclein and α-synuclein in the presence of NbSyn2 are similar, an observation consistent with the chemical shift and $^1D_{NH}$ results, indicating that binding of NbSyn2 does not have a large effect on the overall conformational sampling of α-synuclein. In contrast, binding of NbSyn87 leads to a significant increase in protein rigidity at the C-terminus, revealed by significantly higher values of $^1D_{C\alpha H\alpha}$. This finding agrees well with chemical shift data that indicate increased chain rigidity and $^1D_{NH}$ data that suggest long-range interactions are perturbed. Taken together, these findings strongly support the conclusion that NbSyn87 binding significantly perturbs conformational sampling of the protein.

Our structural results are supported by the different effects of the two nanobodies on the aggregation behavior of α-synuclein in vitro, monitored by dot-blot assays (see Materials and Methods). NbSyn2 does not enhance aggregation when mixed at half-equimolar concentrations with α-synuclein under continuous shaking at 37 °C and has a relatively modest effect even when added at equimolar concentration (Figure 4). By contrast, NbSyn87 readily promotes the aggregation of α-synuclein by decreasing the lag phase and diminishing the half-time of fibril formation at 0.5 and 1 equimolar concentrations; the half-time of aggregation decreases by 5 and 17 h, respectively.

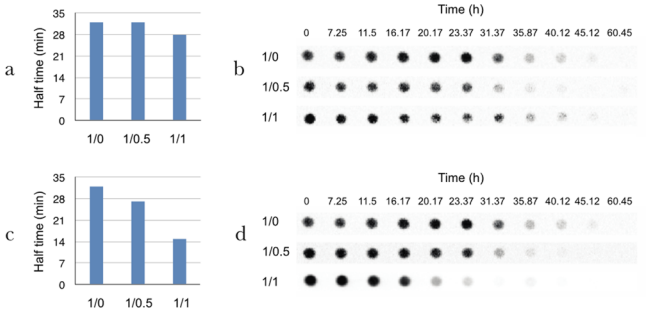

Figure 4. Aggregation of α-synuclein with and without NbSyn2 and NbSyn87. Half of the aggregation time of α-synuclein in the presence of 0 (ratio 1/0), 0.5 (ratio 1/0.5), and 1 (ratio 1/1) equimolar concentration of NbSyn2 (a) or NbSyn87 (c) monitored by dot-blot assays. The decrease in monomer concentration at each time point of the reaction process was also measured by dot-blot assays at the same ratios of nanobodies NbSyn2 (b) and NbSyn87 (d).

CONCLUSIONS

We investigated two camelid single-domain antibodies that influence in distinct ways the structural ensemble of α-synuclein by binding two distinct epitopes within its C-terminal domain. This work has revealed the different roles of two distinct segments of the C-terminal domain of α-synuclein in stabilizing long-range intramolecular interactions and modulating aggregation behavior. These results thus support the view that it may be possible to identify specific binding partners capable of stabilizing α-synuclein in nonpathogenic monomeric states.

AUTHOR INFORMATION

Corresponding Authors

*E-mail: mv245@cam.ac.uk.
*E-mail: cmd44@cam.ac.uk.

Present Address

†T.G.: Healx Ltd., St John's Innovation Centre, Cowley Road, Cambridge CB4 0WS, U.K.

Funding

This work was supported by the Advanced Postdoc Mobility Fellowship, Swiss National Science Foundation (PA00-P3-142121), and the Wellcome Trust.

Notes

The authors declare no competing financial interest.

DOI: 10.1021/acs.biochem.6b00149
Biochemistry 2016, 55, 3116−3122

REFERENCES

(1) Spillantini, M. G., Schmidt, M. L., Lee, V. M.-Y., Trojanowski, J. Q., Jakes, R., and Goedert, M. (1997) α-Synuclein in Lewy bodies. *Nature 388*, 839−840.

(2) Polymeropoulos, M. H., Lavedan, C., Leroy, E., Ide, S. E., Dehejia, A., Dutra, A., Pike, B., Root, H., Rubenstein, J., and Boyer, R. (1997) Mutation in the α-synuclein gene identified in families with Parkinson's disease. *Science 276*, 2045−2047.

(3) Spillantini, M. G., Crowther, R. A., Jakes, R., Hasegawa, M., and Goedert, M. (1998) α-Synuclein in filamentous inclusions of Lewy bodies from Parkinson's disease and dementia with Lewy bodies. *Proc. Natl. Acad. Sci. U. S. A. 95*, 6469−6473.

(4) Baba, M., Nakajo, S., Tu, P. H., Tomita, T., Nakaya, K., Lee, V. M., Trojanowski, J. Q., and Iwatsubo, T. (1998) Aggregation of alpha-synuclein in Lewy bodies of sporadic Parkinson's disease and dementia with Lewy bodies. *Am. J. Pathol. 152*, 879−884.

(5) Galvin, J. E., Lee, V. M., and Trojanowski, J. Q. (2001) Synucleinopathies: clinical and pathological implications. *Arch. Neurol. 58*, 186−190.

(6) Dauer, W., and Przedborski, S. (2003) Parkinson's disease: mechanisms and models. *Neuron 39*, 889−909.

(7) Singleton, A., Farrer, M., Johnson, J., Singleton, A., Hague, S., Kachergus, J., Hulihan, M., Peuralinna, T., Dutra, A., and Nussbaum, R. (2003) α-Synuclein locus triplication causes Parkinson's disease. *Science 302*, 841−841.

(8) Theillet, F.-X., Binolfi, A., Bekei, B., Martorana, A., Rose, H. M., Stuiver, M., Verzini, S., Lorenz, D., van Rossum, M., and Goldfarb, D. (2016) Structural disorder of monomeric α-synuclein persists in mammalian cells. *Nature 530*, 45−50.

(9) Lotharius, J., and Brundin, P. (2002) Pathogenesis of Parkinson's disease: dopamine, vesicles and alpha-synuclein. *Nat. Rev. Neurosci. 3*, 932−942.

(10) Winner, B., Jappelli, R., Maji, S. K., Desplats, P. A., Boyer, L., Aigner, S., Hetzer, C., Loher, T., Vilar, M., Campioni, S., Tzitzilonis, C., Soragni, A., Jessberger, S., Mira, H., Consiglio, A., Pham, E., Masliah, E., Gage, F. H., and Riek, R. (2011) In vivo demonstration that alpha-synuclein oligomers are toxic. *Proc. Natl. Acad. Sci. U. S. A. 108*, 4194−4199.

(11) Cremades, N., Cohen, S. I., Deas, E., Abramov, A. Y., Chen, A. Y., Orte, A., Sandal, M., Clarke, R. W., Dunne, P., and Aprile, F. A. (2012) Direct observation of the interconversion of normal and toxic forms of α-synuclein. *Cell 149*, 1048−1059.

(12) Lashuel, H. A., Overk, C. R., Oueslati, A., and Masliah, E. (2012) The many faces of α-synuclein: from structure and toxicity to therapeutic target. *Nat. Rev. Neurosci. 14*, 38−48.

(13) Toth, G., Gardai, S. J., Zago, W., Bertoncini, C. W., Cremades, N., Roy, S. L., Tambe, M. A., Rochet, J. C., Galvagnion, C., Skibinski, G., Finkbeiner, S., Bova, M., Regnstrom, K., Chiou, S. S., Johnston, J., Callaway, K., Anderson, J. P., Jobling, M. F., Buell, A. K., Yednock, T. A., Knowles, T. P., Vendruscolo, M., Christodoulou, J., Dobson, C. M., Schenk, D., and McConlogue, L. (2014) Targeting the intrinsically disordered structural ensemble of alpha-synuclein by small molecules as a potential therapeutic strategy for Parkinson's disease. *PLoS One 9*, e87133.

(14) Dumoulin, M., Last, A. M., Desmyter, A., Decanniere, K., Canet, D., Larsson, G., Spencer, A., Archer, D. B., Sasse, J., Muyldermans, S., Wyns, L., Redfield, C., Matagne, A., Robinson, C. V., and Dobson, C. M. (2003) A camelid antibody fragment inhibits the formation of amyloid fibrils by human lysozyme. *Nature 424*, 783−788.

(15) De Genst, E. J., Guilliams, T., Wellens, J., O'Day, E. M., Waudby, C. A., Meehan, S., Dumoulin, M., Hsu, S. T., Cremades, N., Verschueren, K. H., Pardon, E., Wyns, L., Steyaert, J., Christodoulou, J., and Dobson, C. M. (2010) Structure and properties of a complex of alpha-synuclein and a single-domain camelid antibody. *J. Mol. Biol. 402*, 326−343.

(16) Kirchhofer, A., Helma, J., Schmidthals, K., Frauer, C., Cui, S., Karcher, A., Pellis, M., Muyldermans, S., Casas-Delucchi, C. S., Cardoso, M. C., Leonhardt, H., Hopfner, K. P., and Rothbauer, U. (2010) Modulation of protein properties in living cells using nanobodies. *Nat. Struct. Mol. Biol. 17*, 133−138.

(17) Messer, A., and Joshi, S. N. (2013) Intrabodies as neuroprotective therapeutics. *Neurotherapeutics 10*, 447−458.

(18) Rissiek, B., Koch-Nolte, F., and Magnus, T. (2014) Nanobodies as modulators of inflammation: potential applications for acute brain injury. *Front. Cell. Neurosci. 8*, 344.

(19) Schenk, D., Barbour, R., Dunn, W., Gordon, G., Grajeda, H., Guido, T., Hu, K., Huang, J., Johnson-Wood, K., Khan, K., Kholodenko, D., Lee, M., Liao, Z., Lieberburg, I., Motter, R., Mutter, L., Soriano, F., Shopp, G., Vasquez, N., Vandevert, C., Walker, S., Wogulis, M., Yednock, T., Games, D., and Seubert, P. (1999) Immunization with amyloid-beta attenuates Alzheimer-disease-like pathology in the PDAPP mouse. *Nature 400*, 173−177.

(20) Harmsen, M. M., and De Haard, H. J. (2007) Properties, production, and applications of camelid single-domain antibody fragments. *Appl. Microbiol. Biotechnol. 77*, 13−22.

(21) Guilliams, T., El-Turk, F., Buell, A. K., O'Day, E. M., Aprile, F. A., Esbjorner, E. K., Vendruscolo, M., Cremades, N., Pardon, E., Wyns, L., Welland, M. E., Steyaert, J., Christodoulou, J., Dobson, C. M., and De Genst, E. (2013) Nanobodies raised against monomeric alpha-synuclein distinguish between fibrils at different maturation stages. *J. Mol. Biol. 425*, 2397−2411.

(22) Delaglio, F., Grzesiek, S., Vuister, G. W., Zhu, G., Pfeifer, J., and Bax, A. (1995) NMRPipe: a multidimensional spectral processing system based on UNIX pipes. *J. Biomol. NMR 6*, 277−293.

(23) Wishart, D. S., and Case, D. A. (2001) Use of chemical shifts in macromolecular structure determination. *Methods Enzymol. 338*, 3−34.

(24) Bertoncini, C. W., Jung, Y. S., Fernandez, C. O., Hoyer, W., Griesinger, C., Jovin, T. M., and Zweckstetter, M. (2005) Release of long-range tertiary interactions potentiates aggregation of natively unstructured alpha-synuclein. *Proc. Natl. Acad. Sci. U. S. A. 102*, 1430−1435.

(25) Skora, L., Cho, M. K., Kim, H. Y., Becker, S., Fernandez, C. O., Blackledge, M., and Zweckstetter, M. (2006) Charge-induced molecular alignment of intrinsically disordered proteins. *Angew. Chem., Int. Ed. 45*, 7012−7015.

(26) Ottiger, M., Delaglio, F., and Bax, A. (1998) Measurement of J and dipolar couplings from simplified two-dimensional NMR spectra. *J. Magn. Reson. 131*, 373−378.

(27) Yang, D., Tolman, J. R., Goto, N. K., and Kay, L. E. (1998) An HNCO-based Pulse Scheme for the Measurement of 13Calpha-1Halpha One-bond Dipolar couplings in 15N, 13C Labeled Proteins. *J. Biomol. NMR 12*, 325−332.

(28) Permi, P. (2003) Measurement of residual dipolar couplings from 1Halpha to 13Calpha and 15N using a simple HNCA-based experiment. *J. Biomol. NMR 27*, 341−349.

(29) Yao, J., Dyson, H. J., and Wright, P. E. (1997) Chemical shift dispersion and secondary structure prediction in unfolded and partly folded proteins. *FEBS Lett. 419*, 285−289.

(30) Berjanskii, M. V., and Wishart, D. S. (2005) A simple method to predict protein flexibility using secondary chemical shifts. *J. Am. Chem. Soc. 127*, 14970−14971.

(31) Camilloni, C., De Simone, A., Vranken, W. F., and Vendruscolo, M. (2012) Determination of secondary structure populations in disordered states of proteins using nuclear magnetic resonance chemical shifts. *Biochemistry 51*, 2224−2231.

(32) Adzhubei, A. A., Sternberg, M. J., and Makarov, A. A. (2013) Polyproline-II helix in proteins: structure and function. *J. Mol. Biol. 425*, 2100−2132.

(33) Apetri, M. M., Maiti, N. C., Zagorski, M. G., Carey, P. R., and Anderson, V. E. (2006) Secondary structure of alpha-synuclein oligomers: characterization by raman and atomic force microscopy. *J. Mol. Biol. 355*, 63−71.

(34) Richardson, J. S., and Richardson, D. C. (2002) Natural beta-sheet proteins use negative design to avoid edge-to-edge aggregation. *Proc. Natl. Acad. Sci. U. S. A. 99*, 2754−2759.

DOI: 10.1021/acs.biochem.6b00149
Biochemistry 2016, 55, 3116−3122

(35) Prestegard, J. H., al-Hashimi, H. M., and Tolman, J. R. (2000) NMR structures of biomolecules using field oriented media and residual dipolar couplings. *Q. Rev. Biophys. 33*, 371−424.
(36) Bernado, P., Bertoncini, C. W., Griesinger, C., Zweckstetter, M., and Blackledge, M. (2005) Defining long-range order and local disorder in native alpha-synuclein using residual dipolar couplings. *J. Am. Chem. Soc. 127*, 17968−17969.
(37) Dedmon, M. M., Lindorff-Larsen, K., Christodoulou, J., Vendruscolo, M., and Dobson, C. M. (2005) Mapping long-range interactions in alpha-synuclein using spin-label NMR and ensemble molecular dynamics simulations. *J. Am. Chem. Soc. 127*, 476−477.
(38) Goddard, T. D., and Kneller, D. G. (2008) *SPARKY 3*, University of California, San Francisco, https://www.cgl.ucsf.edu/home/sparky/.

DOI: 10.1021/acs.biochem.6b00149
Biochemistry 2016, 55, 3116−3122